Low-energy diffuse scattering electron-spin polarization analyzer

J. Unguris, D. T. Pierce, and R. J. Celotta

National Bureau of Standards, Gaithersburg, Maryland 20899

(Received 28 February 1986; accepted for publication 22 March 1986)

A new, compact (approximately fist sized), efficient electron-spin analyzer is described. It is based on low-energy (150 eV) diffuse scattering from a high-Z target, for example, an evaporated polycrystalline Au film opaque to the incident electron beam. By collecting a large solid angle of scattered electrons, a figure of merit $S^2I/I_0 = 10^{-4}$ is achieved with an analyzing power $S = 0.11$. The figure of merit degrades only marginally ($< 10\%$) for beams with an energy width of 40 eV or after one month of operation at 10^{-8} Torr. The electron optical acceptance is of order 100 mm^2 sr eV. The details of the design and construction are discussed and its performance is compared to six other spin analyzers. Illustrative results are presented from an application to scanning electron microscopy with polarization analysis (SEMPA) to image magnetic microstructure.

INTRODUCTION

Electron-based measurements are ubiquitous in most areas of science and technology. An electron is characterized not only by its momentum but also by its spin. However, the use of the spin parameter in measurements made with free electron beams has been greatly hampered by the large experimental inefficiencies present in the preparation of polarized beams and in the measurement of the electron beam polarization. The situation has changed recently for the former case with the advent of a source of polarized electrons[1] which can produce polarized beams with intensities and other characteristics equal to those available from conventional electron guns. Although no breakthrough of similar magnitude has occurred with electron spin polarization analyzers, we describe in this paper a simple, compact and relatively efficient spin polarization analyzer which represents a step in that direction.

Electron-spin polarization measurements have yielded unique information for many types of investigations, from elementary particle interactions at 10 GeV to electron-solid interactions at fractions of an eV. In high-energy physics, the study of parity violation in deep inelastic scattering of polarized electrons on deuterium provided an important experimental test of the unified theory of weak and electromagnetic interactions.[2] At energies of a few eV in electron–atom scattering, the changes in spin polarization of an electron beam scattering from polarized atoms can be used to characterize the interaction in terms of the quantum mechanical amplitudes and phases rather than just a cross section.[3] The measurement of electron-spin polarization has been especially fruitful in investigations of solids[4] and surfaces.[5] For example, the spin polarization of electrons emitted from a ferromagnet either by photoemission, field emission, or secondary emission can be used to characterize the magnetic properties of the material.

Electron-spin polarization measurements also have technological applications. With magnetic storage media of increasingly high density, it is no longer possible to study domain patterns by optical techniques and it becomes necessary to resort to electron microscopy. Fortunately, the secondary electrons generated by a finely focused electron beam retain the spin orientation they had in the domain or magnetic "bit" from which they are emitted.[6] Thus, a spin detector attached to a scanning electron microscope (SEM) allows imaging of the magnetic microstructure of a specimen. The spin detectors we describe here were first used in such an application.[7]

The polarization of an electron beam is the ensemble average of the expectation value of the Pauli spin operator. The statistical mixture of spin states of a partially polarized beam is properly described in the density matrix formalism.[8] The component of the polarization vector along a given direction, for example the z axis, can be written

$$P_z = (N\uparrow - N\downarrow)/(N\uparrow + N\downarrow)\,, \tag{1}$$

where $N\uparrow$ and $N\downarrow$ are the number of electrons with spins, respectively, parallel and antiparallel to the $+z$ direction. The degree of polarization has the range of values $-1 \leqslant P \leqslant 1$.

The exchange interaction and spin-orbit interaction are the origin of the largest electron-spin polarization effects. The exchange interaction arises from the required antisymmetrization of the wave function as specified by the Pauli principle. It is manifested in the scattering of polarized electrons from polarized atoms or from the net spin density in a ferromagnetic surface. In fact, the exchange interaction is the origin of ferromagnetism itself. The spin-orbit interaction arises from the interaction of the electron spin with its own orbital angular momentum. Viewed in the rest frame of the electron as it passes through the electric field of the atom nucleus, the electron sees a magnetic field which interacts with its spin. For scattering from an atom, the spin orbit interaction can be cast in the form[8]

$$V_{so} = \frac{1}{2m^2c^2}\frac{1}{r}\frac{dV(r)}{dr}\,\mathbf{s}\cdot\mathbf{L}, \tag{2}$$

where r is the position of the incident electron with spin $\mathbf{s}$ and angular momentum $\mathbf{L}$. The angular momentum is along the normal to the scattering plane defined by $\hat{n} = (\mathbf{k}\times\mathbf{k}')/|\mathbf{k}\times\mathbf{k}'|$, where $\mathbf{k}$ and $\mathbf{k}'$ are the electron wave vectors before and after scattering, respectively.

The spin-orbit interaction provides the basis of the spin analyzer we describe. In short, for scattering a 100% spin polarized electron beam at a particular scattering angle, we define an asymmetry S

$$S = (I\uparrow - I\downarrow)/(I\uparrow + I\downarrow)\,, \tag{3}$$

where $I\uparrow$ and $I\downarrow$ are the scattered intensities when the spin polarization of the incident beam is, respectively, parallel and antiparallel to the normal to the scattering plane $\hat{n}$. This asymmetry S is usually referred to as the Sherman function when discussing the Mott spin analyzer and will be referred to more generally as the "analyzing power" in our discussion of spin analyzers. It can have the range of values $-1 \leqslant S \leqslant 1$.

Spin analyzers are used in many different applications, and no one type of spin analyzer possesses the characteristics required for every application. We will review the characteristics of analyzers usually considered when evaluating an analyzer for a particular purpose. We will then give a brief historical survey of the major types of analyzers in order to put our new device, which is the subject of this paper, in context.

There are two quantities which are particularly important in quantifying the analyzer characteristics, the figure of merit, and the electron optical acceptance. When the experimental uncertainty is limited by counting statistics, the appropriate figure of merit is $S^2 I/I_0$.[8] Clearly one wants the analyzing power to be as large as possible. The ratio of the detected electrons I to those incident on the spin detector I_0 is also to be optimized. While the figure of merit is a measure of the efficiency with which the analyzer uses the electrons it accepts, a second measure is needed to indicate what fraction of the experimentally generated electrons will be accepted by the analyzing device, i.e., the electron optical acceptance. The spin analyzer's electron optical acceptance should be matched to (i.e., greater than or equal to) the emittance or phase space product of the electron beam to be measured in order to avoid loss of signal. According to the law of Helmholz and Lagrange, at any two points, 1 and 2, along a beam path, the phase space product of the energy E, solid angle $d\Omega$, and cross-sectional area dA is conserved

$$E_1\, dA_1\, d\Omega_1 = E_2\, dA_2\, d\Omega_2\,. \tag{4}$$

In general, a large electron optical acceptance, i.e., a large phase-space product, is a desirable analyzer property, although for any particular experiment nothing is gained once full acceptance of the electron beam is achieved. The maximum acceptable energy spread ΔE of the incident beam may also be a limiting characteristic of the analyzer. Other, somewhat less quantifiable, characteristics of the analyzer need also be considered. The size of the analyzer, which is strongly influenced by the operating energy, can be an important factor. It is desirable that the vacuum requirements of the analyzer and experimental region are compatible, although differential pumping can compensate for significant differences. The long- and short-term stability of the spin analyzer and its calibration are factors which may be strongly related to the vacuum environment. Finally, there is the question of calibration. Some spin analyzers are self-calibrating while others require calibration against another type of analyzer.

The traditional and most widely used means of measuring electron spin polarization is the Mott analyzer. Mott predicted[9] theoretically that the scattering of an electron from a nucleus would depend on the direction of the incident electron's spin if (1) the electron was scattered through an angle greater than 90°, (2) the nucleus from which the electron scattered had a high atomic number Z, and (3) the speed of the electrons approached the speed of light, i.e., electrons with energy greater than 50 keV. This spin dependence, which is due to the spin-orbit interaction, was first observed in 1943 by Shull *et al.*[10] A typical Mott detector operates at 100–120 keV and measures the backscattered electron intensities I_R and I_L at equal angles to the right and left of the beam's incident direction. The degree of polarization along the normal $\hat{n}$ to the scattering plane is then obtained from

$$P_n = A/S, \quad \text{with } A = (I_L - I_R)/(I_L + I_R)\,. \tag{5}$$

The most common configuration detects scattering at $\pm 120°$ from a thin gold foil target. The analyzing power of the foil S is calibrated by measuring the asymmetry for a number of foil thicknesses and extrapolating to zero foil thickness where, from reliable calculations for 100-keV electron scattering from Au nuclei, $S = 0.39$. The value of S is reduced by multiple scattering in thicker foils but the scattering intensity is increased. A reasonable compromise is reached when the value of S ranges from 0.2 to 0.3. The thin Au foils are not opaque to the high-energy electrons. Typically only 10^{-3} to 10^{-4} of the incident electrons are scattered back into the counters.

Low-energy Mott analyzers in which the spin-orbit scattering takes place from a Hg atomic beam have also been used. At these incident energies (< 1000 eV), the high energies "required" for Mott scattering are obtained as the electron passes through the atom's electron cloud and is accelerated toward the nucleus. The Hg beam provides a low-density target leading to lower scattering efficiency. Nevertheless, a figure of merit of 4×10^{-5} has been achieved and it has been suggested that increases may be possible with a higher density Hg beam.[11] Such a spin analyzer requires only moderate vacuum and is well suited to some electron-atom scattering experiments.

A variation of the Mott analyzer has two electrodes inside the vacuum chamber such that the electrons are accelerated to the inner electrode and scattered from the Au foil at high energy and then are decelerated as they pass again to the outer electrode which is at nominal ground potential. This accelerating/decelerating type of analyzer has been realized in cylindrical[12] and spherical geometries.[13,14] It has the advantages that there is good discrimination against inelastically scattered electrons and the scattered electron detectors are operated near ground potential. The chamber is also at ground potential. This type of Mott analyzer in the spherical geometry has operated effectively in the 20–40-keV range with a figure of merit of 2×10^{-5}. Because of its relatively small size for a Mott analyzer, it has been dubbed the "Mini Mott."

When the scattering takes place at low energy from a single crystal, the electrons are diffracted back into well-

defined beams. The left–right asymmetry of the scattering, which is again due to the spin-orbit interaction can be exploited to make a spin analyzer.[15] This polarized low-energy electron diffraction or PLEED analyzer differs from those described thus far in two important respects: (1) the target is opaque to the electrons and (2) the scattering is no longer diffuse. Although a very good figure of merit of 1.6×10^{-4} has been achieved, some of the characteristics of the analyzer may present drawbacks for some applications. To meet the conditions for diffraction with good spin analyzing power, the angular spread of the incident beam at the crystal should be less than 2° and the energy spread less than 5 eV. The alignment of the detector is also critical. The surface of the monocrystal must be atomically clean, which, for the tungsten target used thus far, means flashing to ~2500 K every $\frac{1}{4}$–$\frac{1}{2}$ h.

We mention here three other spin polarization analyzers which, while not as generally applicable as those surveyed above, are useful in certain situations. The spin dependence[16] of Møller scattering,[17] which is due to the Pauli principle, is useful for measuring the longitudinal polarization of high-energy electrons ($\gtrsim$0.3 MeV). Another method is an optical technique[18] where the spin-polarized electrons transfer angular momentum in the excitation of Zn atoms from the $4s^2\ {}^1S_0$ ground state to the $4s5s\ {}^3S_1$ excited state. Analysis of the polarization of the light emitted on subsequent decay of this state determines the polarization of the incident beam. Another type of detector exploits the fact that owing to the spin-orbit interaction, there is a spin dependence in the absorption of a spin polarized electron beam incident at an angle on a metal surface.[19] The observation of this spin dependence is generally enhanced at energies near that where the secondary yield is unity. While such a detector is extremely compact and efficient, it has the drawback for some applications that the signal is inherently an analog signal; the counting of single electron pulses is not possible.

In Sec. I we present a detailed discussion of our new, low-energy, diffuse-scattering spin polarization analyzer, including the design objectives, the basic principles of the spin analyzer, the details of the design and construction, and measurements of its performance. In addition, results from an application of the spin analyzer to scanning electron microscopy will be shown. In Sec. II we compare this new analyzer to several of those reviewed above and present a table of such factors as operating energy, scattering efficiency, figure of merit, electron optical acceptance, size, and vacuum requirements.

I. LOW-ENERGY, DIFFUSE SCATTERING SPIN ANALYZER

A. Design objectives

Because electron-spin polarimeters are used in a wide variety of experimental situations, no single set of design objectives can be rigidly applied. However, there are a few salient design features which have wide applicability. One such feature is that the design be relatively compact. A conventional, high-energy Mott analyzer operating at 100 keV is relatively bulky, typically occupying several cubic meters owing to the required accelerating optics and safety region around the device. In many experiments, such space requirements represent more than an inconvenience. For example, in angle-resolved spectroscopies like angular photoelectron emission or differential electron scattering, the detector is typically rotated around the sample. Since a large spin analyzer is essentially immobile, either the radiation source must be moved or a complex electron optical path must be constructed to bring the electrons emitted into the selected solid angle back to the rotation axis and then on to the stationary polarimeter. In a new method of magnetic domain imaging, a spin polarization analyzer is attached directly to a scanning electron microscope.[7] Here the size and weight of a large spin analyzer could present potentially very difficult problems because of the effect on the vibration isolation techniques used to allow the microscope to achieve very high spatial resolution.

The efficiency of the analyzer system, as measured by the figure-of-merit $S^2 I/I_0$ is an important consideration in spin polarization experiments where the spin effects may be subtle and the polarization to be measured small. We maximize the efficiency of the analyzer by a careful choice of target and operating conditions, to maximize S, and by use of a large collection angle for scattered electrons, to maximize I/I_0. Our goal for the figure of merit was to do as well or better than the best known spin polarization detection systems.

As mentioned above, a detector is also characterized by its electron optical acceptance and the detector design will limit the types of electron sources that can be analyzed without signal loss. We have chosen to design our detector to match small, low-energy sources which have undergone some angular selection. If sources of moderate or high-energy electrons emitted into a large solid angle are to be analyzed, a Mott type analyzer, which achieves a large electron optical acceptance because of its very high analysis energy, may be preferred.

Experiments involving spin analysis are typically very complex. An analyzer which is simple to install and use would be very advantageous. This means that the mechanical and electron optical alignment should be readily accomplished, and the scattering target should be easily generated and remain stable for a length of time longer than a typical experiment, i.e., at least one day. This will depend on the vacuum environment at the detector and in particular on the composition of the residual gases. The design criteria was set at stable operation at pressures lower than 1×10^{-9} Torr for periods of days. Simple differential pumping could be employed to connect the detector to a poorer vacuum.

A further consideration is the accuracy of the polarization measurement as distinct from the precision with which it is made. The theory applicable to detectors operating at the more convenient low energies is not reliable enough to permit an initial calculation of the detectors' analyzing power. Hence, such spin analyzers must be made highly reproducible and stable and calibrated by comparison with an analyzer of high accuracy or a source of known polarization. If the spin analyzer is sufficiently stable, the overall accuracy should be very near that of the calibration standard.

B. Principles of operation

This spin analyzer is based upon the spin-dependent diffuse scattering of 150-eV electrons from an evaporated polycrystalline Au film due to the spin-orbit interaction. Because of the $\mathbf{L}\cdot\mathbf{s}$ dependence of the spin-orbit interaction, the analyzer is sensitive to the transverse components of the spin polarization which are those normal to the scattering plane. A polarization along the incident electron direction, i.e., a longitudinal polarization, will not be detected. A gold-scattering target was selected for the following reasons: (1) the high atomic number of Au leads to a large spin-orbit interaction and, hence, greater analyzing power; (2) the Au film's surface is not as chemically reactive as that of other high-Z materials so that surface contamination is less of a problem; and (3) Au is easily evaporated in a clean, well-defined manner.

The use of an evaporated polycrystalline Au film as the target results in a diffuse, relatively structureless spatial distribution of scattered electrons. A measurement of the angular dependence of the asymmetry and intensity for scattering of 145-eV electrons from a Au film is shown in Fig. 1. These measurements were made by directing electrons from a GaAs polarized electron source at various Au film targets and measuring the scattered electron distributions with a Faraday cup.[20] Angular profiles were also measured with incident electron energies that varied from 100 to 300 eV. The angular profiles showed only smooth, atomiclike variations in intensity and aysmmetry at various beam energies. In contrast, the scattering from a single crystal is extremely sensitive to angle and energy as a result of electron diffraction from the crystal lattice.[20] The total integrated amount of scattering, however, is about the same for polycrystalline and single-crystal samples, only the energy and angular dependencies are very different.

Although the insensitivity of the scattering from the Au film to angle and energy is a distinct advantage, the diffuse nature of the scattering results in very little signal being scattered into any particular direction. One can compensate for this weak scattering by using a detector with a large solid angle acceptance. In our case, we use a microchannel plate followed by a large area anode. The detector, therefore, integrates over the intensity and asymmetry curves shown in Fig. 1.

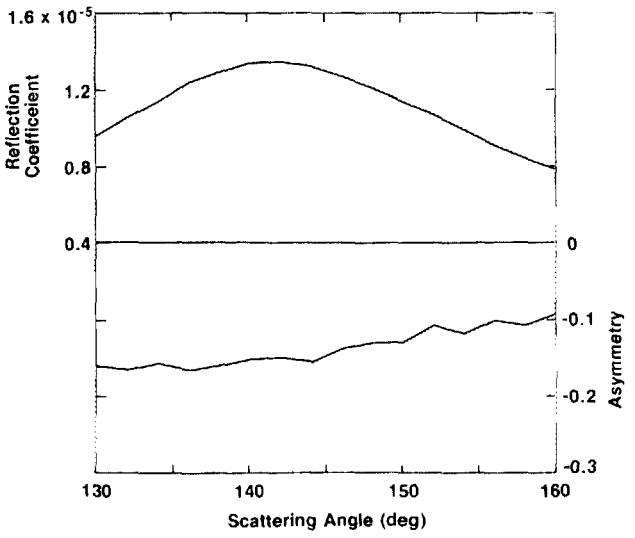

FIG. 1. Angular dependence of the intensity and of the spin-dependent asymmetry for scattering 145-eV electrons from a polycrystalline gold film. The angular resolution of the Faraday cup detector comprised a cone half angle of 1°.

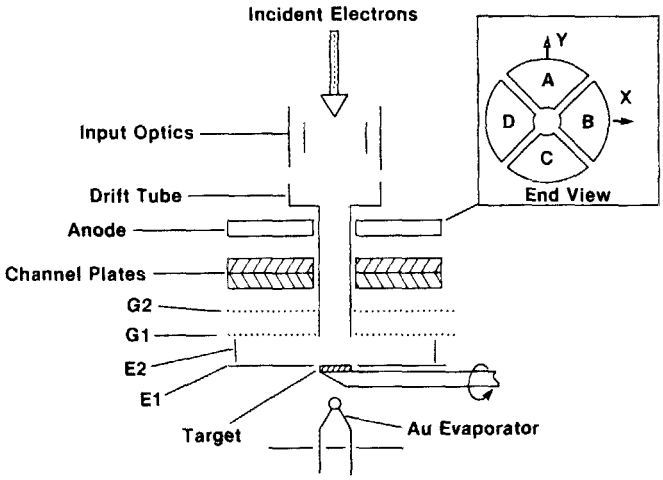

FIG. 2. Schematic of the low-energy diffuse scattering spin analyzer. The inset shows the view of the anode seen by electrons emerging from the channel plate.

C. Analyzer design

A schematic and photograph of this spin analyzer are shown in Figs. 2 and 3, respectively. Electrons to be analyzed arrive at the analyzer by way of input electron optics which couple the detector to the rest of the experimental apparatus. In our case the input optics consist of electrostatic deflection plates which center the electron beam in the analyzer and an energy changing, three element tube lens which focuses the beam on the Au film and changes the energy of the electrons

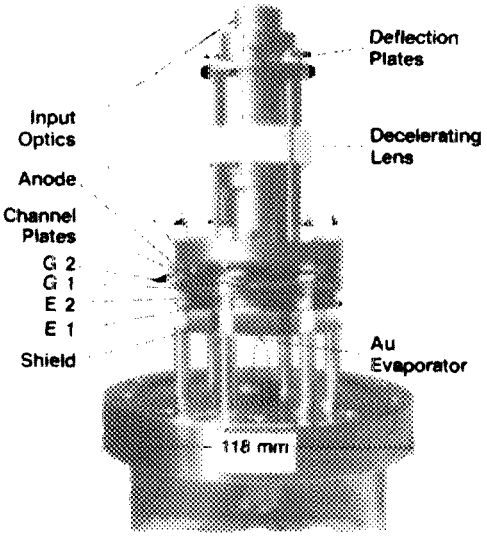

FIG. 3. A photograph of the spin analyzer including input optics appropriate for the scanning electron microscope application. Note the simple layered construction on six posts mounted on the 118-mm-diam flange, which gives the scale.

so that they impinge on the film with 150 eV of kinetic energy. In the scanning electron microscope configuration which will be discussed later, the electron energy change at this lens is from 1500 to 150 eV. Following the input optics is a drift tube which is at the same potential as the Au target. Our drift tube has a 4.78 mm i.d. and a 5.28 mm o.d. and is 14.5 mm long. The tube is wrapped with one layer of 0.076-mm-thick Kapton[21] film to electrically isolate it from the channel plates and grids.

After passing through the drift tube, the electrons strike a Au film target. The targets are made by evaporating an optically opaque film of Au onto a Ta substrate after the vacuum system has reached the 10^{-9} Torr pressure range. The electron scattering characteristics of the Au film are not particlarly sensitive to substrate material or to its preparation. No significant differences were observed between Ta, Mo, or stainless-steel substrates. In addition, the Ta substrates were prepared with various degrees of surface roughness ranging from highly polished to lapped with coarse (240 grit) sand paper. Again no significant differences were observed except for the polished Ta surface which gave more structured angular scattering profiles. Presumably the polished surface permitted larger, single-crystal domains to grow and hence added crystalline diffraction effects to the scattering. To prepare the Ta substrates for the analyzer described here we lapped the surface with 400-grit sand paper. The target is mounted on a rotary feedthrough which permits the target to either face the incoming beam or, by rotating it 180°, face the Au evaporator. The evaporator is of a hairpin type constructed of 0.25-mm-diam tungsten wire with a 40-mg Au bead melted at the tip. In the evaporation position the target is surrounded by a shield which prevented Au from being deposited onto the microchannel plates.

In the present configuration the electrons scatter in a field-free region, since the grid G1 and the electrodes E1 and E2 are all at the Au target potential. Therefore, only those electrons that are elastically backscattered between an angle of 125° and 155° will arrive at the electron multiplier. One possible future variation would be to bias both electrode E2 and the drift tube at a negative potential with respect to the Au target, thereby focusing the scattered electrons into the grids and channel plates and effectively increasing the solid angle acceptance of the electron multiplier.

In yet another possible mode, electrodes E1 and E2 and the Au target could be kept at a sufficiently large negative bias voltage so that the incident electrons do not have sufficient energy to reach the Au surface and instead reflect back into the electron multiplier. This mode would be useful in measuring the total number of electrons incident on the Au target in situations where the full incident electron signal is desired and polarization analysis is not required.

After the grid G1, which is kept at the Au target potential, is a grid G2, which is biased at a negative voltage with respect to the target in order to prevent very low-energy secondary electrons that are generated at the target from reaching the electron multiplier. These secondary electrons do not retain any of the polarization information of the incident electrons and hence degrade the signal. Because the retarding field of the grid system is planar and not radial, the grids do not form a perfect electron energy filter, but respond only to the energy of motion normal to the grids. Therefore, with a typical retarding bias of -40 V applied to G2 with respect to G1, electrons need at least 49 eV of energy to get past G2 near the grid's center and 122 eV at the grid's edge. We expect that somewhat greater efficiency could be achieved with spherical grids at the expense of simplicity of construction. The grids were constructed from stainless-steel mesh (4 wires/mm, 0.025-mm-diam wire) by stretching the mesh over a circular frame (63.5 mm o.d. by 44.5 mm i.d.) which was made from 0.25-mm-thick Ta sheet. The mesh was then spot welded to the frame and a 6.4-mm–diam hole was punched in the center for the drift tube. Improved grids prepared by photochemical machining will be used in subsequent devices.

Electrons that pass the retarding grid are accelerated by several hundred volts into the electron multiplier assembly which amplifies and collects the signal. The multiplier assembly consists of a chevron pair of microchannel plates[22] and a four quadrant anode. The channel plates were provided by the manufacturer with a 6-mm-diam hole in the center for the drift tube. The total voltage across the channel plate assembly is typically between 1000 and 2000 V. In addition, the anode is biased by a positive 200 V with respect to the back of the channel-plate assembly. The anode consists of a circular, 1.16-mm-thick Pyrex plate with a 7.6-mm-diam hole cut in the center and a Au anode pattern evaporated onto it. The anode pattern is shown in the inset of Fig. 2. The four quadrants permit the simultaneous measurement of the incident electron beam's two transverse spin polarization components, P_x and P_y. P_x is given by

$$P_x = \frac{1}{S}\frac{N_A - N_C}{N_A + N_C}, \tag{6}$$

where N_A and N_C are the number of pulses, or the current, measured to anode quadrants A and C, respectively, and S is the analyzing power. Similarly P_y is given by

$$P_y = \frac{1}{S}\frac{N_D - N_B}{N_D + N_B}. \tag{7}$$

The entire assembly, consisting of the evaporator shield, E1, E2, G1, G2, the channel plates, and the anode are all held together by a ceramic post and spacer arrangement that is shown in detail in Fig. 4. There are six of these posts equally spaced around the detector perimeter on a 57.15-mm-diam circle. This diameter was selected because it was the one already used by the channel-plate manufacturer. In order to simplify assembly, we use alumina tubes and spacers that are of standard, commercially available[23] lengths and diameters.

The electronics required to extract and process signals from the polarization analyzer depend to a great extent upon the intensity of the electron beam that is to be analyzed. As with any electron multiplier system, two operating modes are possible: (1) a pulse-counting mode in which the channel plates are run at their maximum gain and the number of pulses arriving at the anode are counted and (2) an analog mode in which the channel plates are run at low gains and the currents to the anodes are measured. At low signal levels,

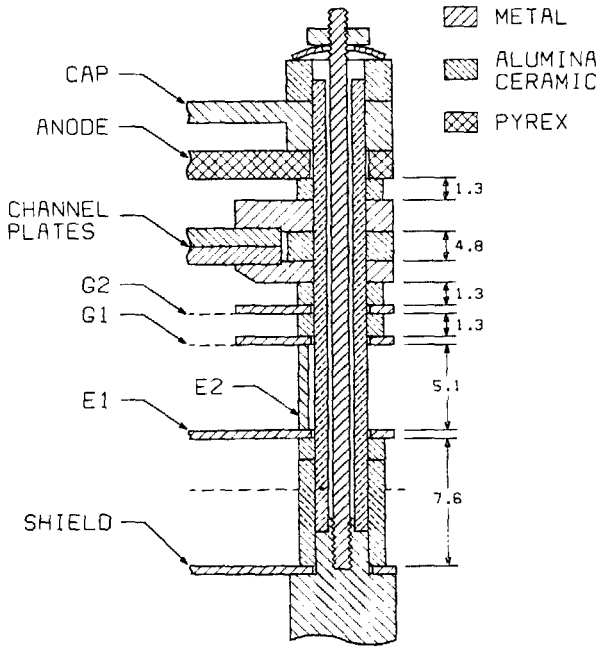

FIG. 4. Detailed drawing with dimensions in millimeters of one of the six support posts visible in Fig. 3.

the pulse-counting mode is used. When the signal level increases to the point that the amplified current approaches 10% of the multiplier bias current, the amplifier gain must be reduced and the analog mode is used. Reducing the gain avoids channel–plate nonlinearities at these high currents.

In fact the nonlinearity problem is especially severe in polarization measurements where one is interested in measuring changes in spin-dependent signals, which are inherently only a very small fraction of the total signal. In practice this means that, for our polarization analyzer with its associated channel-plate characteristics, we switch from pulse to analog modes when the current incident on the Au film becomes greater than 2×10^{-12} A. In the pulse counting mode we first capacitively decouple pulses from the anodes. The pulses then pass through an amplifier followed by a discriminator and are finally counted in a scaler. In the analog mode the current to the anode is measured using a current-to-voltage amplifier which is at the anode potential. The signal is then brought to ground using an isolation amplifier. Both the pulse-counting and analog techniques have been used successfully with the polarization analyzer.

D. Analyzer performance

The Au film polarization analyzer operating characteristics and calibration were determined by using a negative electron affinity GaAs source[1] which produces an electron beam of known intensity, energy, and polarization. The detector's performance for a wide range of incident electron currents and energies could, therefore, be studied. In addition, the polarization of the electron source is easily reversible so that non-spin-dependent apparatus asymmetries could be accounted for. Unless specified, the following conditions held for these measurements: (1) The analyzer was operated in an analog mode with the channel-plate gain adjusted so that the anode current was 8×10^{-8} A or less; (2) G1, E2, E1, and the target were at the same potential; (3) the energy of the electrons at the Au target was 150 eV; and (4) G2 was biased at -50 V with respect to G1.

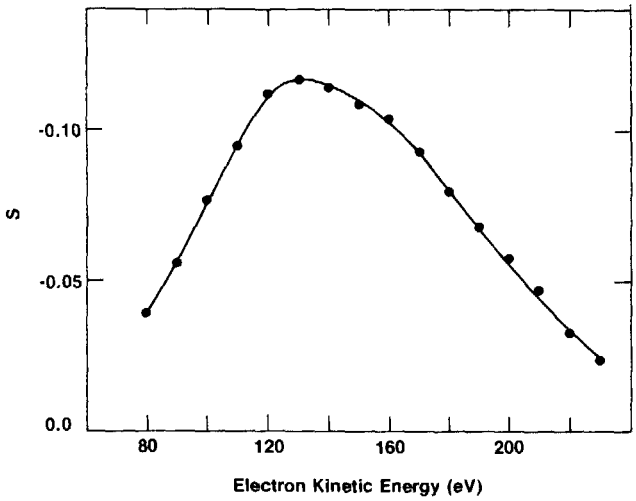

FIG. 5. Analyzing power S as a function of kinetic energy of the electron beam on the gold film target.

Figure 5 shows how the analyzing power of the analyzer varies as the energy of the incident electron beam is changed while keeping the analyzer voltages fixed at their 150-eV operating settings. By integrating the data in Fig. 5 we can measure the detector's response to beams with larger energy spreads than that from the GaAs source. Figure 6 shows the resulting figure of merit for an electron beam with a 150-eV mean energy and an energy width of ΔE (FWHM). From these measurements we see that the detector is not particularly sensitive to either variations in the incident electron mean energy or in its energy spread.

To understand how electrons that are inelastically scattered from the Au film affect the detector's performance, the analyzing power and scattered intensity were measured as a function of the bias voltage G2. The measured analyzing power and normalized intensity are shown in Fig. 7, and the corresponding figure of merit is shown in Fig. 8. While keep-

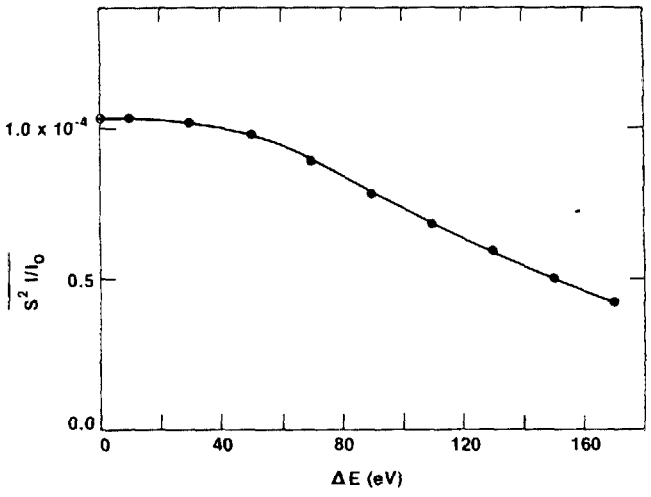

FIG. 6. The figure of merit $S^2 I/I_0$ determined as a function of energy spread of the incident electron beam.

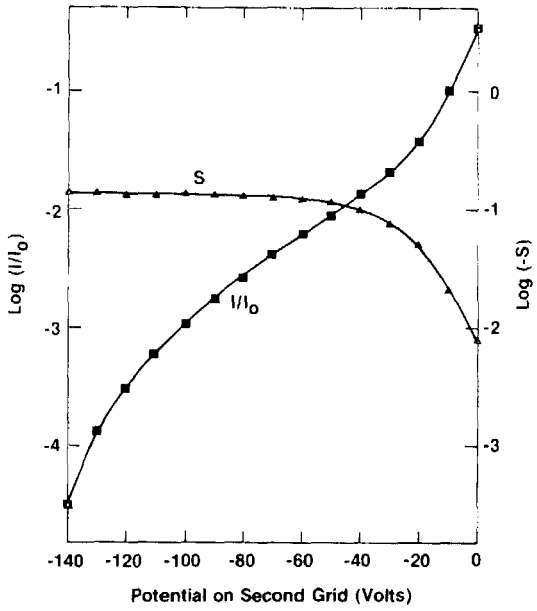

FIG. 7. The analyzing power and normalized scattered intensity are shown for 150-eV incident electrons in the analyzer of Figs. 2 and 3 as a function of the potential or the second grid G2 measured with respect to the gold film target.

ing in mind that the flat grids are not true energy filters, this data indicates that only the lowest energy inelastically scattered electrons have no useable polarization information and hence degrade the signal. Inelastically scattered electrons with energies greater than approximately 40 eV are useful in measuring polarization.

The long-term reproducibility of the polarization analyzer was measured by repeatedly measuring the analyzing power of the detector operating in its standard configuration of 150-eV incident electrons and -50-V retarding bias on G2. Measurements were made over a two-month time span during which several new Au films were evaporated, and the analyzer was operated in various modes. During this time the average resolving power for an analyzer with a clean Au film was 0.107 ± 0.004. The precision of each individual measurement was typically ± 0.001. Similar monitoring of a second identically constructed polarization analyzer gave an average resolving power of 0.102 ± 0.003.

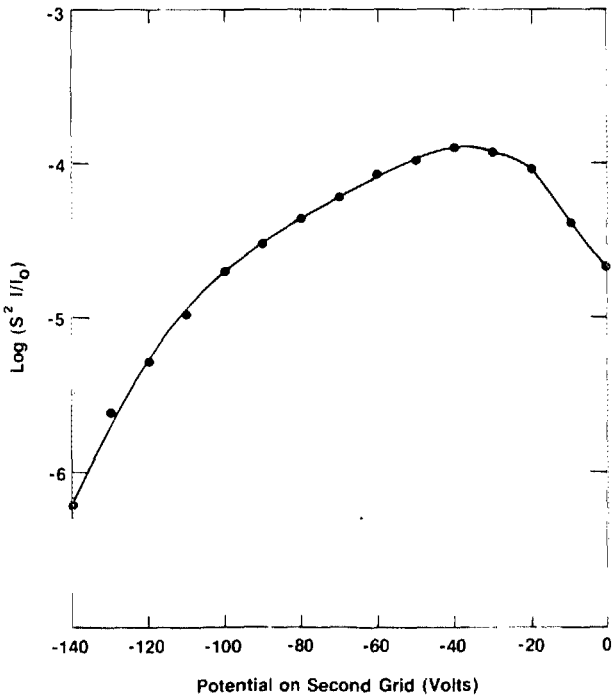

FIG. 8. The figure of merit calculated from the data of Fig. 7.

We studied the sensitivity of the detector to surface contamination by monitoring the analyzing power as a function of time after evaporating a fresh Au film. With the ultrahigh-vacuum chamber at its base pressure of 2×10^{-10} Torr, only a small, approximately 5% decrease in the analyzing power would occur over the week following the evaporation of a new Au film. Following this, the detector characteristics would not change significantly for several weeks. We cannot say whether these observed changes were due to surface contamination or some structural relaxation of the Au film. As a more severe contamination test, we intentionally exposed the detector to an air leak which kept the vacuum chamber at 1×10^{-7} Torr for 90 h. This exposure reduced the analyzing power by 10%. Assuming that the contamination was simply proportional to the integrated gas flux, this result would mean that the analyzer could be operated for over a month at a pressure of 1×10^{-8} Torr or, if necessary, for about an hour at a pressure of 1×10^{-5} Torr and only suffer a 10% loss of analyzing power. Measurements were also made for the most extreme case of Au films that were exposed to atmosphere for several days. In this case the analyzing power was reduced to 0.03. The exact reason for the decay of the analyzing power with air exposure is not known; however, Auger scans of similar air-exposed films indicated that small amounts of C, N, and O were present on these surfaces. In any case, evaporating a new Au film on the substrate brought the detector quickly back to its optimum operating conditions.

E. Application: SEMPA

Although there are many potential uses of this new type of polarization analyzer, the devices described in this paper were particularly designed for measuring the spin polarization of secondary electrons that are generated during scanning electron microscope (SEM) imaging of magnetic surfaces.[7] Since the secondary electrons excited by the primary electron beam retain the polarization they had in the magnetic solid, polarization measurement provides a direct way of measuring and, hence, imaging the magnetic microstructure in the region probed by the SEM. A major advantage of these spin analyzers in this application is their small size, which makes adding them to the SEM straightforward. No major modifications of the SEM or its operation were required. A schematic of the SEM with polarization analyzers is shown in Fig. 9. We use a UHV SEM with a field emission electron source to excite the specimen. Secondary electrons are collected by accelerating them by 1500 eV into the collection optics. Most of the secondaries then pass through an energy analyzer whose sole function in the magnetic imaging mode is to filter out high-energy elastically scattered elec-

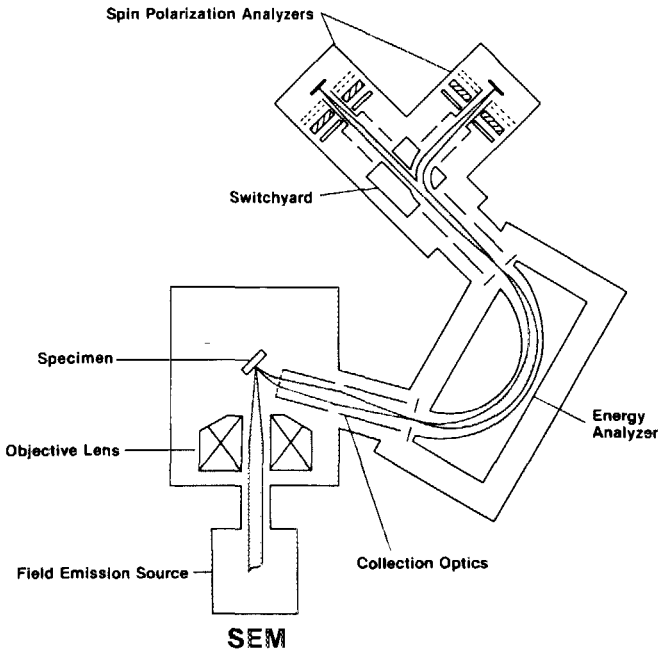

FIG. 9. A schematic view of the scanning electron microscope with two orthogonal spin analyzers to measure all three components of the electron spin polarization.

trons from the specimen. Following the energy analyzer are two orthogonal Au film spin polarization analyzers. Since a single detector can only measure the two transverse components of the polarization, electrostatic right-angle deflection of the beam is required to transform the longitudinal polarization component into a transverse one that can then be measured by the second spin analyzer. The multiple detectors give the scanning electron microscopy with polarization analysis (SEMPA) technique[7] the unique capability of being able to map both the relative magnitude and the direction of the magnetization vector. An additional important feature is that the intensity and polarization are measured simultaneously and independently, thus permitting the separation of magnetic images from topographic ones. An example of a magnetic microstructure image obtained using SEMPA is shown in Fig. 10. These 128×128 pixel images were obtained in about 15 min. The intensity photo shows the gradual decrease in the field-emission gun intensity during the scan as well as surface topographic features such as scratches and precipitatelike point defects. The polarization image shows three magnetic domains. Comparison of the two images shows how the defects pinned the domain wall between two large domains and created a third smaller domain.

II. COMPARISON OF SPIN ANALYZERS

As mentioned in the Introduction, there are several types of spin analyzers with widely varying characteristics which may make a particular one of them most appropriate for some specific application. Having discussed in detail the design and construction of the low-energy diffuse scattering electron-spin polarization analyzer, in this section we compare its parameters with those of six other spin analyzers as summarized in Table I. We shall discuss each of the columns of the table and some specific entries as warranted.

The spin analyzers divide on the basis of operating energy into the three operating at many keV and the four operating at less than 200 eV. The operating energy is closely correlated with size. The entries in the size column are intended as order of magnitude values. The entry for size depends on the particular construction and the reader is referred to the references to make a more detailed comparison. A typical Mott analyzer with the scattering chamber at 100 kV and the safety region around it will occupy several cubic meters. Even the much smaller cylindrical and spherical retarding field types have a high-voltage feedthrough and typically occupy, including the safety region, more than 0.1 m^3. The low-energy spin analyzers are much smaller; the compact spin analyzer discussed in this paper occupies about 10^{-3} m^3.

Because the spin dependence in the scattering is due to the spin orbit interaction, all of the targets are high atomic number materials such as W, Au, and Hg, with $Z = 74$, 79, and 80, respectively. The high-energy analyzers use thin Au foils which are extremely fragile, especially if not backed (i.e., supported by a low-Z material like Formvar). Because of the high operating energy, such analyzers are not sensitive to surface contamination and can operate in a vacuum of

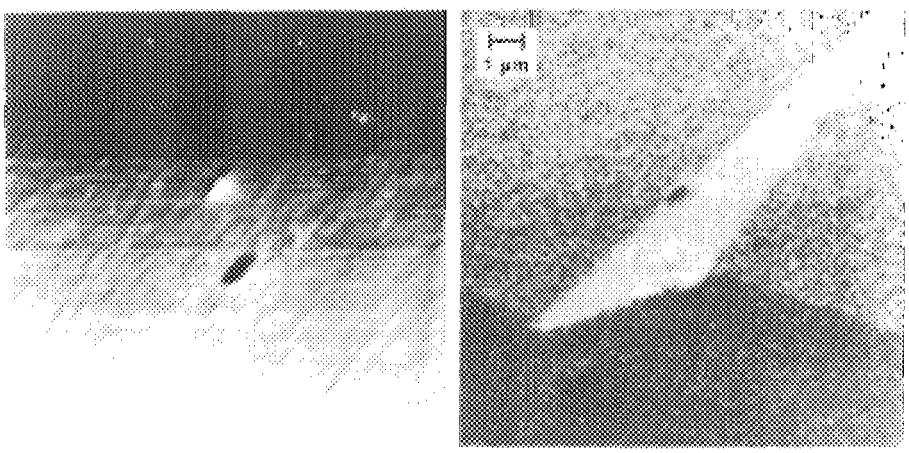

FIG. 10. An illustrative SEMPA image shows one component of the electron spin polarization on the right and the intensity on the left. Three topographical features believed to be due to precipitates in this Fe-3% Si crystal are visible in the intensity image. Three different magnetization regions are evident in the gray scale of the polarization image. The dagger-shaped domain appears to have walls pinned at the crystal defects.

TABLE I. Comparison of spin analyzers.

Analyzer type	Operating energy	Size m^3	Target	Vacuum required	ΔE	$EA\Omega$ mm^2 sr eV	I/I_0	S	Figure of merit	Ref.
Mott, traditional	100–120 keV	1–10	Thin Au foil	10^{-5}	10 keV	10^3	1.5×10^{-3}	0.26	1×10^{-4}	24
Mott, cylindrical retarding	60–120 keV	10^{-1}	Thin Au foil	10^{-5}	1.3 keV	10^4	10^{-6}	0.33	1×10^{-7}	12
Mott, spherical retarding	20 keV 40 keV	10^{-1}	Thin Au foil	10^{-5}	1.3 keV	10^4	1.4×10^{-3} 4×10^{-4}	0.12 0.20	2×10^{-5}	13,14
Hg beam	15 eV	10^{-3}	Hg atoms	10^{-5}	2 eV	10	2.8×10^{-4}	0.37	4×10^{-5}	11
PLEED	105 eV	10^{-3}	W crysatal	10^{-10}	2 eV	1.6	2.2×10^{-3}	0.27	1.6×10^{-4}	15
Absorbed current	100 eV	10^{-4}	Au film	10^{-9}	10 eV	1			1×10^{-4}	19
Low-energy diffuse scattering	150 eV	10^{-3}	Au film	10^{-9}	40 eV	10^2	0.9×10^{-2}	0.11	1×10^{-4}	this work

10^{-5} Torr, but they can also be operated, if required, in ultrahigh vacuum. The Hg beam spin analyzer, on the other hand, is inherently a low-vacuum device and would require significant differential pumping if it were part of an experiment that took place in ultrahigh vacuum. The other three spin analyzers are inherently ultrahigh-vacuum devices although the PLEED spin analyzer using a W single crystal is much more sensitive to contamination than the two analyzers employing evaporated Au films.

The allowable energy spread ΔE of a beam of electrons such that the polarization of the beam can be measured by a given spin analyzer may be limited by different factors. In the traditional Mott analyzer, the analyzing power S varies slowly with beam energy. The energy spread of the incident beam is limited by the 10-keV energy window of the surface barrier Si detectors; electrons with energy more than 10 keV below the nominal beam energy will not be detected. In the retarding field Mott analyzers, the window of electron energies that are detected is variable from a very small value, such that only elastically scattered electrons are detected, to much larger values. A large energy window allows more inelastically scattered electrons to be detected which improves the efficiency I/I_0 at the expense of S. An optimum figure of merit was found for a 1.3-keV analyzer energy window, which places a similar limitation on the energy spread of the incident beam. At low energies, the analyzing power varies more rapidly with beam energy. The acceptable energy spread for the low-energy spin analyzers is limited by the scattering conditions which produce high analyzing powers. The values of ΔE for the Hg analyzer[11] operating at 15 eV and for the PLEED[15] analyzer are, therefore, a few eV. For the analyzer described in this work, S varies less rapidly with energy than in the diffraction analyzer and an energy spread ΔE of 40 eV is acceptable.

The electron optical acceptance, or phase space product $EA\Omega$ varies widely between spin analyzers. The high energy of a traditional Mott analyzer increases its electron optical acceptance enormously. In such an analyzer, a typical beam diameter on an Au foil scattering target would be 3 mm with an angular spread of about 1°. A well-collimated beam that fills the defining apertures eliminates movement of the beam on the Au foil which can otherwise be a major source of error in such an analyzer. A representative value for the acceptance of a traditional Mott analyzer[24] is 10^3 mm^2 sr eV.

The cylindrical and spherical Mott analyzer focus the beam to the foil. The symmetry of the electric field is such as to greatly reduce displacements of the beam on the foil that would lead to spurious asymmetries. We estimate the acceptance phase space by calculating the maximum angle an electron can have with respect to the axis at a particular operating energy and with beam-defining apertures as in Ref. 13. Such an electron has a nonradial (i.e., transverse) component of velocity which, in the time the electron is accelerated toward the inner sphere, displaces the electron beam such that it no longer passes through the aperture in the inner sphere. In this manner, $EA\Omega$ is estimated to be 10^4 mm^2 sr eV for the spherical Mott analyzer operating at 30 keV. A comparable order of magnitude is estimated for the cylindrical Mott analyzer operating at 100 keV, where the higher energy is offset by the fact that the electron beam in this geometry is focused in only one dimension. Realistic ray tracing calculations for these geometries would be of interest for an accurate determination of $EA\Omega$, but these estimates are sufficient for the present purpose.

The Hg beam spin analyzer accepts electrons scattered at angles from 85° to 110°; the analyzing power remains high over this range.[25] Thus one expects that an incident beam could have a solid angle of 0.5 sr and still be accepted by the spin analyzer. This leads to the rather substantial $EA\Omega$ for this low-energy detector of order 10 mm^2 sr eV.

The parameters of the absorbed current detector[19] are very sensitive to incident angles. In general, the factors entering the phase space product are about the same for the absorbed current detector and the PLEED detector[15] which also has severe constraints on the angular range of the incident beam.

The low-energy diffuse scattering spin analyzer has an electron optical acceptance of 10^2 mm^2 sr eV in the embodiment specified in this paper. Since a range of scattering angles is detected there is not the restrictive constraint on the angular spread of the beam to be analyzed as in the absorbed current detector or PLEED detector. An acceptance half-angle of 10° and an area of 16 mm^2 are achieved for this new spin analyzer.

While the most frequently quoted parameter is the figure of merit, $S^2 I/I_0$, the actual values of S and I/I_0 which go into the figure of merit are also of importance. If S is small and the polarization to be determined is small, the apparatus asymmetries and other systematic uncertainties must be particularly well controlled. Several spin analyzers achieve a

figure of merit of approximately 10^{-4}. This represents the current state of the art.

The figure of merit is related to other parameters such as the phase space product $EA\Omega$ and energy spread of the beam ΔE. For example, a high figure of merit is achieved in the PLEED spin analyzer when it is operating at a well-defined energy and angle. At somewhat different operating conditions,[26] the PLEED analyzer phase space product could probably be increased a factor of 6 by doubling A and increasing Ω by a factor of 3 but this would be at the cost of reducing the analyzing power possibly to 0.20 from 0.27. In the case of the retarding field analyzers, the large acceptance refers to getting the incident beam to the Au foil target. However, the efficiency I/I_0 is decreased by the retardation which has the effect of enlarging the solid angle of scattered electrons subtended by the inner aperture to a solid angle much greater than that subtended by the electron multiplier at the outer sphere. Improved efficiency should be possible by employing large area detectors at the outer sphere.

Clearly there are pitfalls in simply comparing figures of merit without considering other factors such as the acceptance phase space of the analyzer and the allowable energy spread. A spin analyzer must be matched to the experiment; otherwise the I_0 incident on the analyzer target may be considerably smaller than the current of electrons to be measured.

Surveying these different analyzers, we see a variety of devices, each with its special attributes. Among the most recently developed analyzers there seems to be a trend towards compactness. We believe that the new analyzer described in this work is very competitive with existing spin analyzers and superior for many applications.

ACKNOWLEDGMENTS

We wish to thank Chris E. Kuyatt for his help in designing the electron optics. This work was supported in part by the Office of Naval Research.

[1]D. T. Pierce, R. J. Celotta, G.-C. Wang, W. N. Unertl, A. Galejs, C. E. Kuyatt, and S. R. Mielczarek, Rev. Sci. Instrum. **51**, 478 (1980).
[2]C. Y. Prescott, W. B. Atwood, R. L. A. Cottrell, H. DeStaebler, E. L. Gaswin, A. Gonidec, R. H. Miller, L. S. Rochester, T. Sato, D. J. Sherden, C. K. Sinclair, S. Stein, R. E. Taylor, J. E. Clendenin, V. W. Hughes, N. Sasao, K. P. Schüler, M. G. Borghini, K. Lübelsmeyer, and W. Jentschke, Phys. Lett. **77B**, 347 (1978).
[3]W. Wübker, R. Mollenkamp, and J. Kessler, Phys, Rev. Lett. **49**, 272 (1982).
[4]H. C. Siegmann, F. Meier, M. Erbudak, and M. Landolt, Adv. Electron. Phys. **62**, 1 (1984).
[5]*Polarized Electrons in Surface Physics*, edited by R. Feder (World Scientific, Singapore, 1985).
[6]J. Unguris, D. T. Pirece, A. Galejs, and R. J.Celotta, Phys. Rev. Lett. **49**, 72 (1982).
[7]J. Unguris, G. G. Hembree, R. J. Celotta, and D. T. Pierce, J. Microscopy **139** RP1, (1985).
[8]J. Kessler, *Polarized Electrons*, 2nd edition (Springer, Berlin, 1985).
[9]N. F. Mott, Proc. R. Soc. (London) A **124**, 425 (1929); A **135**, 429 (1932).
[10]L. G. Schull, C. T. Chase, and F. E. Myers, Phys. Rev. **63**, 29 (1943).
[11]K. Jost, F. Kaussen, and J. Kessler, J. Phys. E **14**, 735 (1981).
[12]L. A. Hodge, T. J. Moravec, F. B. Dunning, and G. K. Walters, Rev. Sci. Instrum. **50**, 5 (1979).
[13]L. G. Gray, M. W. Hart, F. B. Dunning, and G. K. Walters, Rev. Sci. Instrum. **55**, 88 (1984).
[14]D. M. Campbell, C. Hermann, G. Lampel, and R. Owen, J. Phys. E **18**, 664 (1985).
[15]J. Kirschner and R. Feder, Phys. Rev. Lett. **42**, 1008 (1979); J. Kirschner, *Polarized Electrons at Surfaces* (Springer, Berlin, 1985), p. 62.
[16]A. M. Bincer, Phys. Rev. **107**, 1434 (1957); G. W. Ford and C. J. Mullin, Phys. Rev. **108**, 477 (1957).
[17]C. Møller, Ann. Phys. **14**, 531 (1932).
[18]M. Eminyan and G. Lampel, Phys. Rev. Lett. **45**, 1171 (1980).
[19]D. T. Pierce, S. M. Girvin, J. Unguris, and R. J. Celotta, Rev. Sci. Instrum. **52**, 1437 (1981).
[20]D. T. Pierce and R. J. Celotta, *Advances in Electronics and Electron Physics*, Vol. 36 (Academic, New York, 1981), p. 219.
[21]Kapton is the trade name of an insulating material available from DuPont, Wilmington, DE. Certain commercial equipment, instruments, or materials are identified in this paper in order to adequately specify the experimental procedure. Such identification does not imply recommendation or endorsement by the National Bureau of Standards, nor does it imply that the materials or equipment identified are necessarily the best available for the purpose.
[22]Model 3040, manufactured by Galileo Electro-Optics, Sturbridge, MA.
[23]Kimball Physics Inc., Wilton, NH.
[24]E. Kisker, R. Clauberg, and W. Gudat, Rev. Sci. Instrum. **53**, 1137 (1982).
[25]G. F. Hanne, K. J. Kollath, W. Wubker, J. Phys. B **13**, L395 (1980).
[26]J. Kirschner (private communication).